Wafer Inspection Technology Challenges for ULSI Manufacturing

Stan Stokowski and Mehdi Vaez-Iravani

KLA-Tencor, One Technology Drive, Milpitas, CA 95035

The use of wafer inspection systems in managing semiconductor manufacturing yields is described. These systems now detect defects of size as small as 40 nm. Some high-speed systems have achieved 200-mm diameter wafer throughputs of 150 wafers per hour. The particular technologies involved are presented. Extensions of these technologies to meet the requirements of manufacturing integrated circuits with smaller structures on larger wafers are discussed.

INTRODUCTION

Wafer inspection systems help semiconductor manufacturers increase and maintain integrated circuit (IC) chip yields. The manufacturers buy these systems at a rate of about $700 million per year. This capital investment attests to the value of these systems in manufacturing IC chips.

The IC industry employs inspection systems to detect defects that occur during the manufacturing process. Their main purpose is to monitor whether the process is under control. If it isn't, the system should indicate the source of the problem, which the manager of the IC fabrication process (fab manager) can fix. The important inspection system characteristics here are defect detection sensitivity and wafer throughput. As we discuss later, sensitivity and throughput are coupled such that greater sensitivity usually means lower throughput. There are both physical and economic reasons for this relationship.

The relative value of sensitivity and throughput depends on the function of the inspection system. There are three general functional requirements for these systems: first, detecting and classifying defects in process development, second, in monitoring a process line, and third, in monitoring a station. In process development one is willing to have low throughput in order to capture smaller defects and a greater range of defect types. However, in monitoring a production line or a station, cost-of-ownership (COO), thus throughput, becomes relatively more important. In this case, of course, the sensitivity must be adequate to capture the yield-limiting defects.

Evolution of the semiconductor manufacturing industry is placing ever greater demands on yield management and in particular, on metrology and inspection systems. Critical dimensions are shrinking to 0.13 µm and 0.10 µm in the near future. Wafer size is increasing from 200 mm to 300 mm. Economics is driving the industry to decrease the time for achieving high-yield, high-value production. Thus, minimizing the total time from detecting a yield problem to fixing it determines the return-on-investment for the semiconductor fabricator.

Thus, inspection systems are evolving from stand-alone "tools" that just found defects to a part of a more complete solution where detecting defects, classifying them, analyzing these results and recommending corrective action are their functions. We do not have space here to consider and review all aspects of yield management systems, which are nevertheless important. Thus, we concentrate on the front end of this process, which is the detection phase, and briefly on classification. In this paper we describe the physical laws and engineering system constraints that determine what an inspection system can do.

HISTORICAL PERSPECTIVE

In the 1970's and early 1980's manual inspection was the norm. Critical dimensions were micrometers and yield limiting defects were easily seen visually. However, production yields were low and their rate of increase slow. Furthermore, the variance in the inspection process was considerable, thus, the desire for automated inspection.

Two types of inspection tools appeared in the early 1980's. One type was an automated microscope that captured bright-field images of patterned wafers and looked for defects by comparing die images (die-to-die comparison). The inspection rate was about 0.1 100-mm diameter wafers per hour (wph). About the same time a tool that detected particles on bare silicon wafers became available. This tool found particles by detecting laser light scattered from the particle, commonly designated in microscopy as dark-field. Its inspection rate was quite rapid at the time, equivalent to about 30 100-mm wph. Its minimum detectable dielectric particle diameter was about 3 µm.

A large difference between the bright field and dark field approaches is that in the latter, one typically has a situation in which the average size of the detected defect is much smaller than the resolution of the optical system. This is why dark-field systems have higher throughput.

Over the ensuing years these inspection tools became more sensitive and faster. In the mid 1980's several

companies introduced dark-field tools that measured defects and particles on patterned wafers. Inspection rates for 200-mm wafers reached 100 wph for unpatterned wafers and 30 wph for patterned wafers. Sensitivity for detecting particles and defects was now sub-micron.

In the early 1990's the bright field tools became more sensitive with higher resolution microscope objectives, and used both cell-to-cell comparisons for array regions of the die, and die-to-die comparisons for logic regions. Throughput increased dramatically with the use of time-delay-integration (TDI) detectors. The detector pixel rate was 100 million pixels per sec (Mpps) and the image processing computer ran at the same rate. For a pixel size of 0.39 µm the tool ran at a 200-mm wafer inspection rate of 1 wph. Sensitivity to defects was about the same as the pixel size.

The year 1995 saw the appearance of a fast scanning-electron-beam microscope (SEM) for inspection. It had a spot diameter of 100 nm and a pixel rate of 12.5 Mpps, which is equivalent to a throughput of 0.05 wph. It also had the capability for inspecting 300-mm wafers, the first system to accomplish this.

This very brief and extremely condensed history brings us to the present capabilities of inspection systems. Bright field systems now use broad-band visible light illumination and high magnification objectives (resolution of 0.4 µm). The pixel rate is 400-600 Mpps with throughputs in the range of 1 to 8 wph, depending on pixel size.

Dark-field systems have achieved a sensitivity of 60 nm (polystyrene spheres on bare silicon) at 50 wph and 150 nm defects on patterned wafers at 30 wph.

Defect review, classification, and analysis are now being integrated to decrease the time for correcting yield problems.

INSPECTION SYSTEM BASICS

To understand how inspection systems will meet industry requirements in the future, we now consider some of the basic physics, engineering, and economic constraints imposed on these systems.

Physics

To inspect an object we look at it via some interrogating means, which are usually photons or electrons scattered by the object. The detected scattered photons or electrons as a function of position (an image) hopefully contains the information needed to determine whether a defect is present. An image processing system then decides if there is a defect. Thus, defect detection naturally consists of three main steps: first, obtaining the image, second, processing the image, and third, applying criteria to this processed image to detect defects.

We find it interesting to compare inspection technology with that of lithography, in particular, the exposure process. Lithography is almost exclusively optical (I-line [365 nm wavelength], deep ultraviolet [DUV, 248 nm] , 193 nm, and eventually extreme ultraviolet [EUV, 13 nm]). The print rate of optical lithography is about 10^{10} resolution elements per sec now and is increasing to 10^{11} over the next few years. This high print rate, of course, is a consequence of the massive parallelism of optical techniques. On the other hand, the highest inspection rate currently is 6×10^{8} pixels per sec. However, optical lithography has an easier task in that it does not have to process and analyze an image.

The challenge for inspection tools is then to detect small defects with a system resolution spot size much larger than the defect size. Fortunately, as we shall see, one does not have to "resolve" a defect in order to detect it. Resolution, appropriately, does impact defect classification and identification. However, again even for performing these functions, we can sometimes obtain sufficient information without necessarily "resolving" the defect.

Even the first step of obtaining the image, by its nature, includes an optical processing step. How we illuminate and collect the resultant scattered light determines the contrast between a defect and the background in which it resides (surface or pattern scattering). Ideally one wants to maximize this contrast by judicially choosing the optical arrangement. Fortunately there are tools and techniques for accomplishing this choice. We describe some of them in this paper. In addition, for periodic array cells optical spatial filtering is effective. Finally light polarization plays an extremely important role in enhancing sensitivity.

This paper concentrates on optical techniques for wafer inspection because they are most commonly used. However, before we describe these techniques in more detail, it is worth looking at the differences between an optical, or photon, system and an e-beam system for inspection. These differences are in the scattering process itself and in the image contrast.

Electron scattering occurs near the surface of the inspected object and thus, a SEM inspector looks at the surface morphology. Also because electric fields affect electron trajectories a SEM inspector can look for electrical defects.

Next, the throughput and sensitivity of the SEM system depends on its resolution and detected electron current. Typically the detected electron current is in the range of 25 nanoamps or more importantly, 10^{11} electrons per second. In a typical dark-field optical system the electron current at the photocathode of a photo-multiplier tube is in the range of 10^{8} to 10^{14} electrons per second The contrast in a SEM system is in the range of 10%-50% whereas in a dark-field optical system the contrast varies from 10% to 10^{6}%. Thus, a dark field optical system has an inherent contrast advantage that translates into a throughput advantage.

A SEM inspector, however, does have very high sensitivity because of its 100 nm resolution and it can detect electrical defects, which an optical system can not do.

Bright-field and dark-field systems

All optical inspection systems depend on photon scattering from the inspected object. Bright-field systems collect both the scattered and reflected light through the same aperture to obtain an image. In addition, one illuminates the object through the objective aperture. Basically these systems are a high-speed microscope. Dark-field systems, on the other hand, only collect the scattered light; no part of the reflected light falls within the collection angle. They can have a multiplicity of configurations, depending on the angle and type of illumination, collection angles, and detector type.

We categorize dark field systems into two main groups: single dark field and double dark field. Single dark field occurs when either the illumination or the collection angle is greater than 45°; double dark field, when both the illumination and collection angle are >45°. As we shall see later, these definitions have their origin in the angular dependence of surface scattering. Figure 1 shows schematically single dark field optics and double dark field optics. This figure also shows two different methods of obtaining an image: the single dark field system using a TDI detector and the double dark field system using a scanner, such as an acousto-optic deflector (AOD), coupled with a PMT detector.

All these systems have their advantages and disadvantages for detecting different defect types. In general, dark field systems are particularly useful when the defect has some high-spatial-frequency topography, whereas bright field is good at finding planar defects. In most cases dark field systems find defects much smaller than the system resolution or spot size; whereas, in bright-field systems the detected defects are about the same size as the system resolution. This fact has important implications for system throughput. However, of particular importance for system sensitivity is the fact that *no one optical arrangement is optimum for detecting all possible defect types*.

Particle scattering

Particles or their effects are the source of a majority of defects in IC chips. Thus, understanding particle scattering

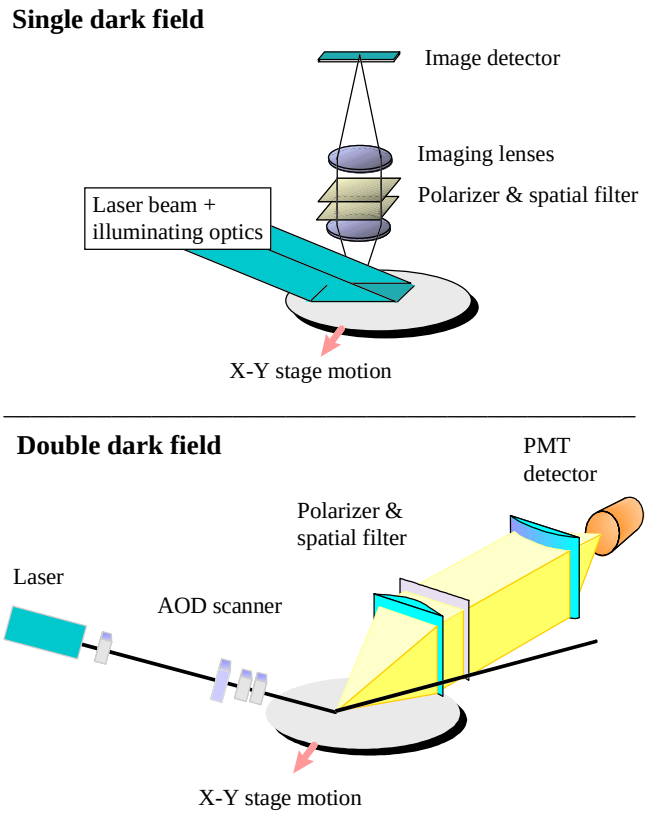

FIGURE 1. Schematics of a single dark-field configuration and a double dark-field configuration.

helps to design sensitive inspection tools. We have a program that calculates scattering from a sphere on a layered substrate when illuminated by a plane wave. It uses a formalism developed by Bobbert and Vleiger (1). Assi (2) and Stokowski et al.(3) developed application software that calculates the polarized scattering into the 2π hemisphere above the substrate. We used this software tool to calculate the scattering patterns shown in this paper, unless otherwise stated.

In Fig. 2 we show our definition of the spherical coordinates that we use in discussing scattering from particles, surfaces and defects. The polar angle is defined from the surface normal and the azimuthal angle counter-clockwise from the reflected beam projected on to the surface plane. The illumination polarization definitions are *s* (E perpendicular to the incidence plane) and *p* (E parallel to the incidence plane). The scattered field polarization is s or p relative to the plane containing the surface normal and the scattered light direction. When talking about polarized scattering, we use subscripts to refer first to the incident polarization and second to the scattered polarization; for example, E_{sp} refers to the p-polarized scattered far field with s-polarized light incident.

To understand some of the basic scattering rules we start with a polystyrene latex sphere (PSL) on silicon. Although PSL spheres are not found in IC fabs, they are convenient

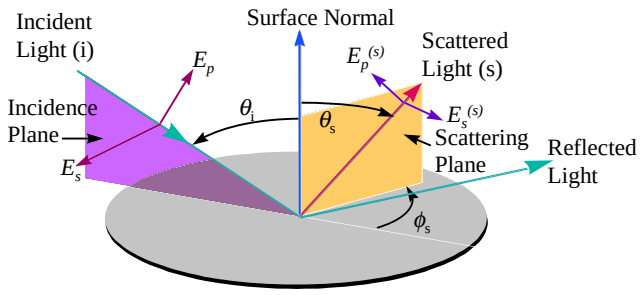

FIGURE 2. Diagram for coordinate and polarization definitions.

for calibrating inspection systems because they are spheres of known diameter.

Figure 3 shows scattering from PSL spheres as a function of diameter, polarization, and angle of incidence. Of particular interest is the advantage of using p-polarized light for detecting small particles. The total scattering cross section for a 60 nm PSL sphere with p-polarized illumination at 70° incident angle is 86 times that with s-polarized light and 42 times that with normal incidence. Also note that most of the scattered light under oblique p-polarized illumination is in the polar angular range of 20° to 70°. Thus, an optimum system for detecting small particles uses obliquely incident p-polarized light and collects the scattered light over a large solid angle, 20° to 70° in polar angle and almost 360° in azimuth.

The advantage of p polarization for small particle detection is a consequence of the standing E-M wave fields above a surface. We can best describe this effect by realizing that for a small enough particle, the particle acts as a probe of the near field because the far-field scattering depends on the E-M field present at the particle. If the particle is small enough, it does not perturb substantially the field that would be present in the absence of the particle.

For 70° incidence Fig. 4 shows the electric field as a function of distance above a silicon surface for s and p polarization. Note that s-polarized light has a low field at the surface ("dark fringe"), whereas, p-polarized light is at a maximum. It follows then that small particle scattering is greatest for p polarization.

Experimental results confirm the utility of the scattering model we use. For example, Figs. 5 and 6 show the agreement between measurements and modeling results for two types of collectors as a function of incidence angle and polarization. One collector covers polar angles from about 25° to 72° and the other from about 6° to 20°, with almost 360° in azimuth.

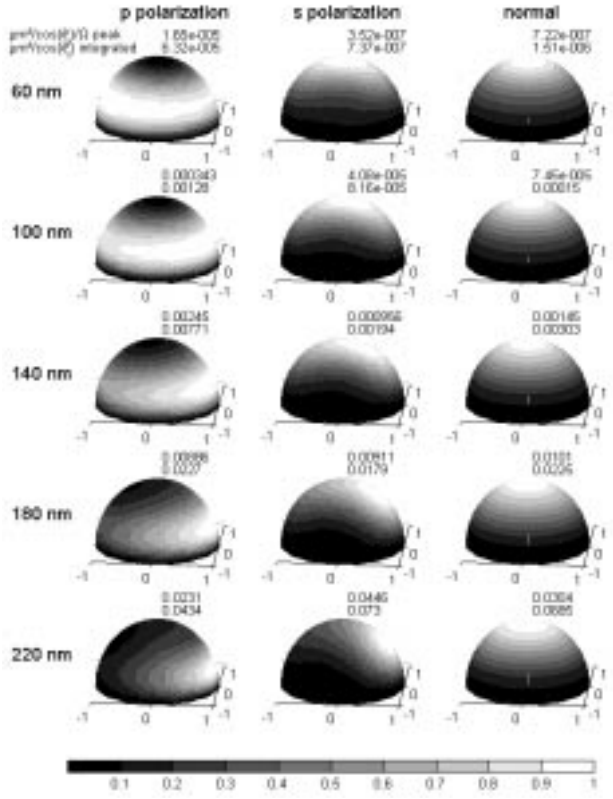

FIGURE 3. Scattered intensity patterns of PSL spheres on silicon as a function of diameter, polarization, and incidence angle. The 488-nm plane wave comes in from the left at 70° incidence and view is about -90° in azimuth from the incidence plane. The last column of images is for normal incidence, circular polarization. The numbers correspond to the peak differential cross sections and the total integrated cross sections in μm² divided by the cosine of the incidence angle.

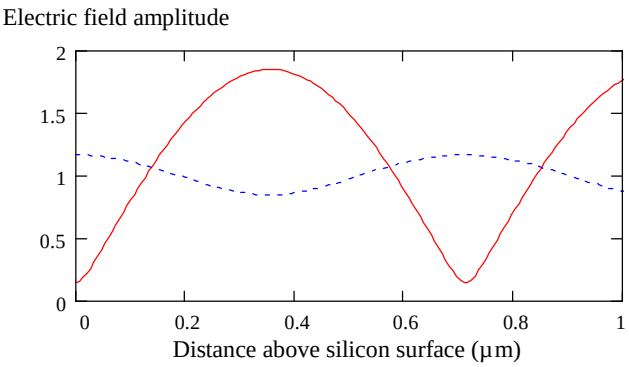

FIGURE 4. Magnitude of the electric field as a function of distance above a silicon surface for s polarization (solid line) and p polarization (dashed line) for 70° incidence and a input field amplitude of 1.

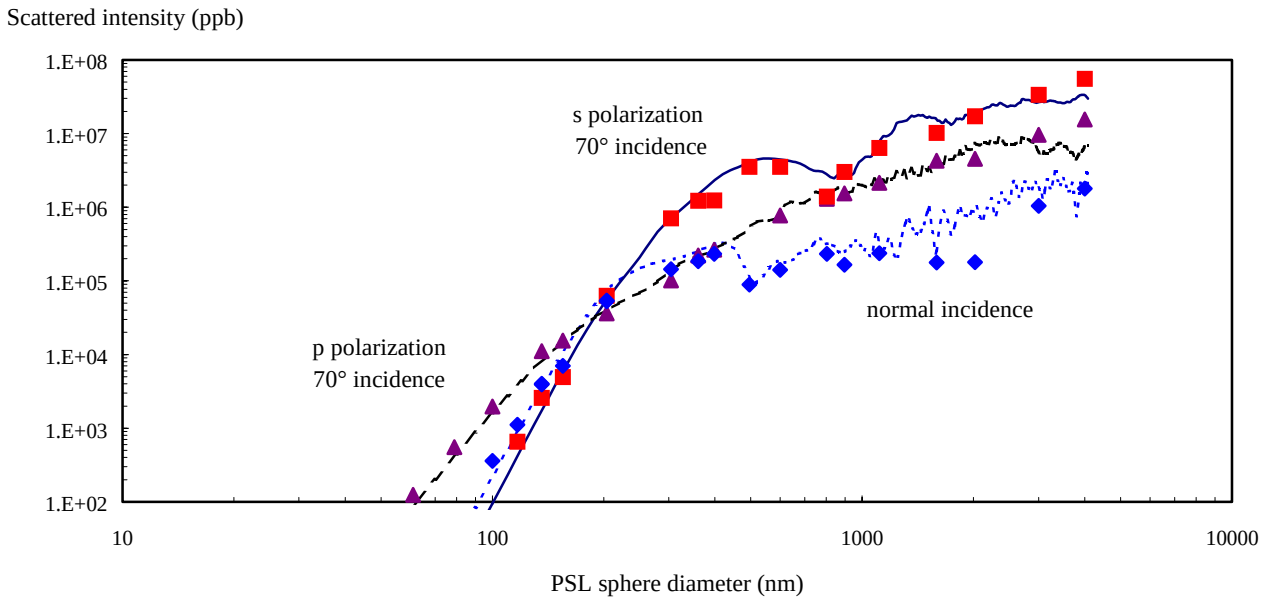

FIGURE 5. Scattering model calculations agree with measurements for PSL spheres on silicon with 70° incidence angle, s polarization (squares) and p polarization (triangles), and normal incidence (diamonds). The collector covers the polar angles from about 25° to 72° and nearly 360° in azimuth.

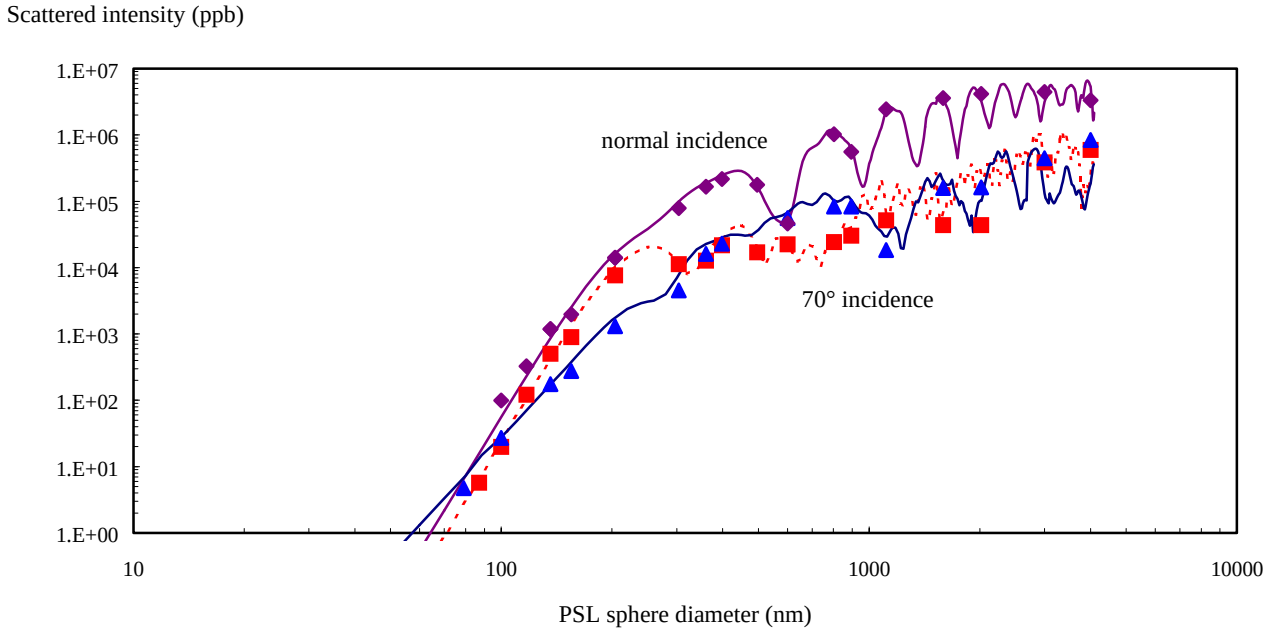

FIGURE 6 Scattering model calculations agree with measurements for PSL spheres on silicon with 70° incidence angle, s (squares) and p (triangles) polarization, and normal (diamonds) incidence. The collector covers the polar angles from about 6° to 20° and 360° in azimuth.

The sensitivity of an inspection system for small particle detection depends on the particle material. In the Rayleigh limit the total integrated scattering of a sphere in a medium depends on

$$\frac{d^6}{\lambda^4}\cdot\left|\frac{(n^2-1)}{(n^2+2)}\right|^2\cdot|E|^2 \qquad (1)$$

where d is the sphere diameter, λ is the illuminating wavelength, n is the refractive index of the sphere and E is the electric field at the sphere (4). Thus, higher refractive index materials, such as semiconductors and metals, scatter more light. Figure 7 compares the total integrated scattering (TIS) for PSL, silicon, and aluminum spheres on silicon. As a consequence, if a system can detect 60 nm PSL spheres on silicon, it can detect 40 nm aluminum spheres on silicon.

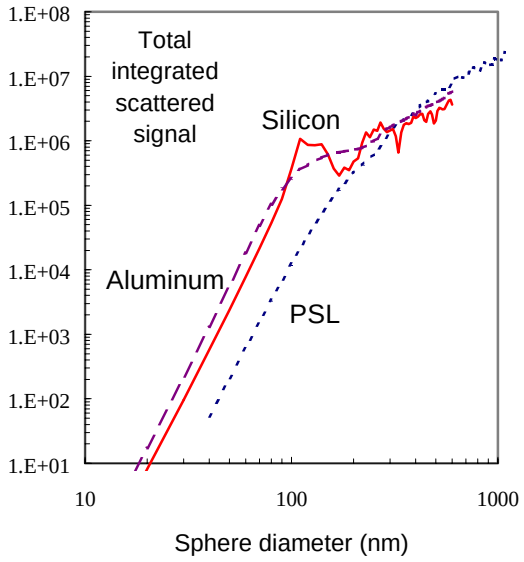

FIGURE 7. Total integrated scattering cross sections for PSL (dotted line), silicon (solid line), and aluminum (dashed line) spheres on silicon.

Particle sizing is always of interest. Typically the industry uses PSL spheres as a calibration standard. If an inspection system uses the total scattered light intensity as an indication of particle size, Figs. 5 and 6 reveal a problem: the intensity is not a monotonic function of the sphere diameter. (Oblique incidence has less of a problem than normal incidence.) Furthermore, the scattered intensity from spheres of other materials obviously do not relate in a simple fashion to the PSL sphere response unless one compares the curves for sphere diameters less than 100 nm. To obtain better sizing one needs to use more than one configuration or mode as suggested, for example, by the responses shown in Figs. 5 and 6.

Surface Scattering

For unpatterned wafers the background noise comes from surface scattering. There are several references that describe surface scattering in great detail; for example, Church et al (5) and Stover (6). We will only describe here the key parameters that determine surface scattering.

For surfaces that are rough, but with height variations much less than the light wavelength, the scattered power per unit solid angle as a function of the polar angle and azimuth is:

$$\frac{dP}{d\Omega} = P_i \cdot \frac{16\pi^2}{\lambda^4} \cdot \left[\cos(\theta_i) \cdot \cos^2(\theta_s) \cdot Q_{p,q}(\theta_i, \theta_s, \phi_s)\right] \cdot PSD(f_x, f_y) \quad (2)$$

where P_i is the input power, $d\Omega$ is the differential solid angle, θ_i, θ_s, ϕ_s are defined in Fig. 2, $Q_{ij}(\theta_i, \theta_s, \phi_s)$ is the polarization factor and $PSD(f_x, f_y)$ is the power spectral density of the surface height variation as a function of the x and y components of the surface spatial frequency. The frequency components, f_x and f_y, are, in turn, related to the scattering angles through the diffraction equations.

Cutting through all this detail, the "bottom line" is: once the surface PSD characteristic is known, we can calculate, to a good approximation, the angular distribution of the light scattered by the surface.

Obviously one tries to minimize surface scattering if one is to obtain good defect sensitivity on rough surfaces. Of particular importance is the polarization factor of Eqn. 2. Figure 8 shows the variation of this factor for silicon over the full scattering hemisphere for the four combinations of input and scattered polarizations and 70° incidence. To minimize surface scattering using the ss polarization combination and collecting light in the vicinity of 90° and 270° azimuth is very effective. In addition, depending on the underlying material the pp polarization combination and collecting scattered light in the forward direction is useful.

In eqn. 2 we can also see that the $\cos(\theta_i)$ and $\cos^2(\theta_s)$ terms also imply that greater sensitivity to detecting particles is obtained in the double dark field configuration, where both angles are >45°.

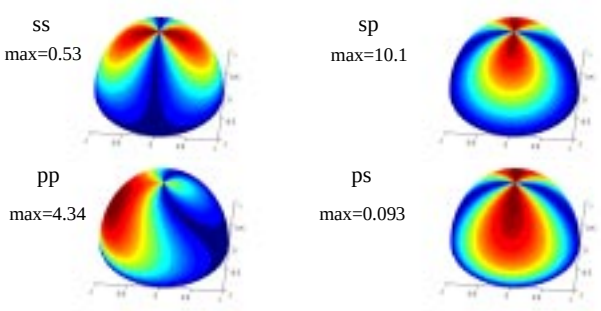

FIGURE 8. Relative magnitudes of the optical polarization factors $Q_{i,j}\cdot\cos^2(\theta)$ for 70° incidence on silicon: ss, pp, sp, and ps polarization combinations over the scattering hemisphere. (Gray scale converted from color: bright band contour is 0.5 of the maximum.) The 488-nm plane wave comes in from the left; view is near -90° in azimuth from the incidence plane.

Unpatterned inspection systems measure the background scattering level, which the industry refers to as "haze". The measured haze value obviously depends on where in the

hemisphere we collect the scattered light. Obviously haze is related to the PSD characteristics of a surface, but the relationship is not necessarily a simple one.

Pit scattering

Pits are of great interest to the silicon wafer manufacturers. Pits have been a problem for inspection systems because they also scatter light and are indistinguishable from particles in a single channel detection system. The wafer manufacturers need to classify pits and particles on silicon wafers. Pits are octahedral voids in Czochralski-grown silicon that have been exposed at the surface by the polishing process. They are also known as "crystal-originated particles" (COP), obviously a misnomer. They sometimes are a single pit and, in a large number of cases, partially overlapping double pits.

Pits and scratches are "surface-breaking" defects; i.e., they are into the surface. The scattering characteristics, therefore, of pits and particles are different and as a consequence, we can classify detected defects as pits or particles if we have information from multiple channels or modes.

The first difference between pits and particles comes from their responses to normal and oblique illumination. Figure 9 is a simple cartoon of this difference. Part a shows the normal illumination with a sphere on a surface intercepting a cross section of the beam. Part b is the condition for an oblique beam where the illuminated area on the surface is the same as Part a. Note that in this plane the same-sized sphere intercepts a larger fraction of the incident beam cross section. Thus, a sphere will scatter significantly more with oblique incidence (see Fig. 3). However, Part c shows that in oblique incidence a pit is at a significant disadvantage relative to a sphere on the surface for scattering light. Thus, comparing the scattered light in normal and oblique incidence can classify pits and particles.

A more important difference between pits and particles is the angular pattern of the scattering. Both theoretical calculations and experimental results show that particles scatter light principally into the polar angle range from 20° to 70° when illuminated with p-polarized light. In contrast, pits scatter primarily toward the normal; therefore, comparing the light scattered into higher angles with those toward the normal will also classify pits and particles. Even for normal incidence this separation works; however, oblique incidence works best. We show experimental results for the p-polarized oblique incidence case in Fig. 10

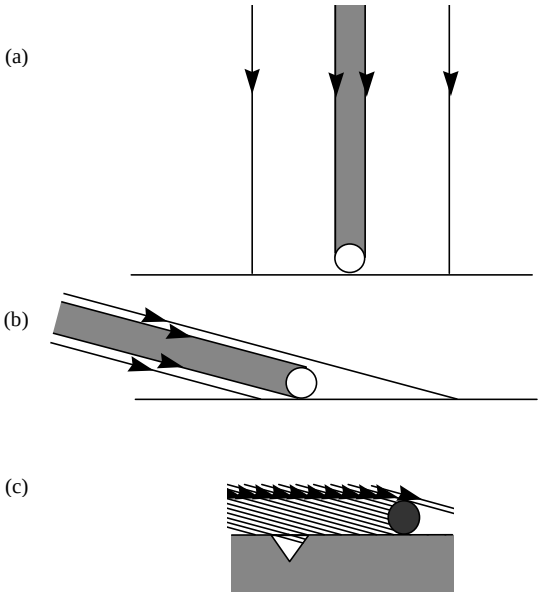

FIGURE 9. Schematic illustrating the difference between particles and pits relative to the illumination incidence angle.

Scratch scattering

Scratches are important in CMP processes and may be yield-limiting. Scratches preferentially scatter perpendicular to their long dimension. Of course, real scratches are not perfect linear defects; in many cases they have cross-sectional variations along the scratch, may have particulate debris nearby, and commonly are "chatter marks." These "chatter marks" or "micro-scratches" actually are a series of short small scratches along a line perpendicular to the long dimension of the scratches.

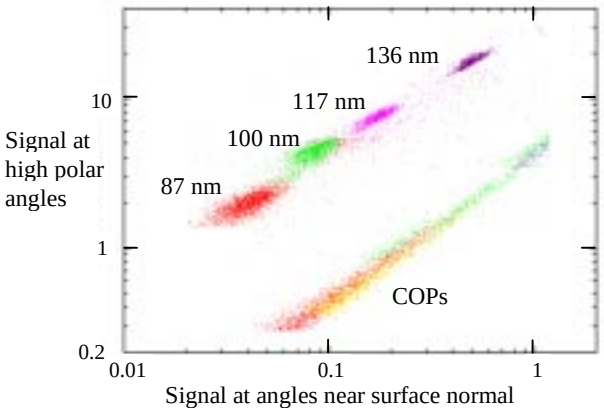

FIGURE 10. Signal levels of PSL spheres and silicon pits with about 25° to 72° collection vs. about 6° to 20° collection, showing the ease of classification.

Scratches also scatter primarily toward the normal, similar to pits. Furthermore, for uniformly detecting scratches of any orientation, normal incidence is preferred.

Dielectric film effects

On patterned wafers dielectric films are present. These lead to a couple of complications. One is the interference effect that produces color under broad band illumination and contrast variation under monochromatic illumination. These effects are particularly troublesome if the film thickness is not uniform and one is trying to do a die-to-die comparison. In bright field systems broad band illumination has helped. In dark field systems circularly polarized light is extremely useful in minimizing the film effect.

As a simple example of this we show the scattering cross section of a PSL sphere on silicon dioxide on aluminum as a function of the oxide thickness in Fig. 11. Note the substantial variations of total scattered light with film thickness with both s and p polarization with oblique incidence. However, because the s and p scattering are out-of-phase with respect to each other, scattering with circular polarization, which has both, is much less affected by film non-uniformity. For normal incidence, of course, s, p, and circular are all equivalent and the film effect is worse than that seen with oblique incidence.

Digs and scratch detection will also be affected by dielectric film thickness and polarization, but their variation in scattering is not in phase with the particle scattered intensity.

Previous layer defects

One may want to see or not see previous layer defects, depending on the system application. Usually for monitoring equipment one does not want to see down into the previous layers. Oblique illumination with s polarization has much less penetration of energy through transparent dielectrics than normal illumination and thus is preferred for detecting current layer defects.

System considerations

An inspection system obtains an image (electron or photon), then processes it to determine if a defect is present, classifies it according to some criteria, and finally passes the information on to a yield management system. Each of these steps may have certain limitations and we describe briefly some of the system considerations.

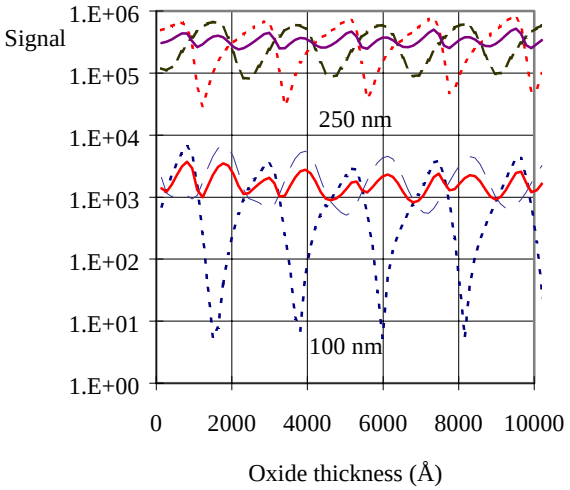

FIGURE 11. Scattered intensity for a 100 nm PSL sphere and a 250 nm PSL sphere on silicon dioxide on aluminum as a function of oxide thickness and input polarization, p polarization (long dash), s polarization (short dash), and circular polarization (solid). Scattered light collected from about 25° to 72° polar angle.

Ideally an inspection system should have high sensitivity, high throughput, and low cost of ownership (COO). However, all these desired system characteristics are coupled and one must do trade-offs to achieve the optimum system.

The semiconductor industry is shrinking the area density of devices by 40% per year. The challenge for the companies developing inspection systems is to maintain image acquisition time and COO constant while going to higher and higher image resolution. We consider how image acquisition, image processing, and defect classification might meet this challenge.

Obtaining the image

Image acquisition is the first step in the inspection process. It consists of illuminating the wafer with a source (lamp or laser), imaging or collecting the scattered light, and detecting this light with a photo-detector (PMT, TDI, or CCD). The source has to be bright enough to provide sufficient photo-electrons from the detector to obtain a reasonable signal-to-noise ratio (S/N). In the case of unpatterned wafers S/N should be about 8 to 10 for 95% capture probability and one false count per 200-mm wafer.

The source in bright field systems is usually a high-pressure mercury (mercury-argon) arc lamp, whereas dark field systems use lasers. The recent development of reliable solid-state, diode-pumped lasers of > 1 Watt power has provided inspection systems with sufficient power for most inspection tasks.

Image acquisition by existing inspection systems fall into one of two main categories: imaging systems or scanner

systems. In imaging systems the source optics illuminates the inspected area, which microscope optics then image on to a TDI or CCD camera. In a scanning system a focused laser beam "paints" the inspected area and a single element detector (usually a PMT) detects the collected scattered light (ref. Fig. 1).

These two types of systems have their own advantages. An imager is basically a fast optical microscope; thus, the optical system design is straightforward. A TDI or CCD camera obtains the image elements in a parallel fashion. A scanner-type system has no constraints on the angles over which one collects the scattered light because it is a non-imaging system. It obtains the image in a serial fashion. An imaging system is useable in a bright-field or single dark field configuration, but not with double dark field. A scanner can have all three configurations. Its disadvantage is the high speed required for the scanner, the detector and its electronics.

At this time we need to describe the relationship between various terms commonly used in inspection systems, such as pixel size, spot size, and system spot size. In a camera-based system pixel size, as referenced to the wafer surface, is the detector element size divided by the magnification of the collection optics from the wafer to the detector. Note that this definition has nothing to do with the resolution of the objective lens. In a scanner system the focused Gaussian spot size is the full width between the e^{-2} points. Obviously in this case the resolution of the focusing optics determines the spot size. For these systems the pixel size is the spot size divided by the number of electronic samples per e^{-2} width.

The sensitivity of an inspection system is related to the system spot size, which includes the resolution, or modulation transfer function, of the optics, the detector element size, the front-end electronic bandwidth, and convolutions done after digitization. In addition, noise limits sensitivity; noise sources include photo-electron shot-noise, detector noise, electronic noise, noise from the analog-to-digital converter (ADC), aliasing noise, and spatial quantitization noise. These last two noise sources depend on the spatial sampling frequency relative to the system spot size. Generally one increases sensitivity by decreasing the system spot size.

Note that system spot size is a governing factor in sensitivity, *not* pixel size.

Throughput of an inspection system on the other hand is inversely related to the *square* of the pixel size. Thus, the time for actually inspecting the wafer is determined by the pixel rate of an inspection system, given its pixel size. Additional time affecting throughput is taken by operations such as wafer loading and unloading, alignment and registration, and data processing.

Fig. 12 shows the relationship between pixel size and inspection time for different pixel rates. Clearly one tries to use as large a pixel as one can while achieving a given sensitivity. Here is where dark field systems have a great advantage over bright field systems; the system spot size to defect size ratio is considerably greater than 1 in dark field systems, whereas bright field system have a ratio closer to 1. For example, albeit, a particularly advantageous situation, a dark field system exists that can detect small PSL spheres on bare silicon with a defect-to-spot area ratio of 3×10^5.

The detector or scanner is limited in speed. For imaging systems the fastest ones employ TDI detectors with 400-600 Mpps. The fastest scanners use AOD technology, currently running at an equivalent pixel rate of about 50 Mpps. However, the slower pixel rate in a scanning system is more than compensated by the larger defect to pixel size ratio in a dark field configuration.

Processing the image

After obtaining the image, the image processor has to determine the presence of a defect and to accomplish this function at a rate almost as large as that for the front-end detection. In a simple unpatterned wafer inspection system a simple threshold scheme works well. However, die-to-die and/or cell-to-cell comparisons are required for patterned wafers.

For DRAM chips with their highly periodic structures some inspection systems use optical spatial filtering to eliminate the light scattered from the periodic structure before it reaches the detector. Thus, only light scattered by the non-periodic defects is detected. This technique only works with coherent laser illumination. Optical filtering typically lowers the background scattering from the array by 100 times or greater.

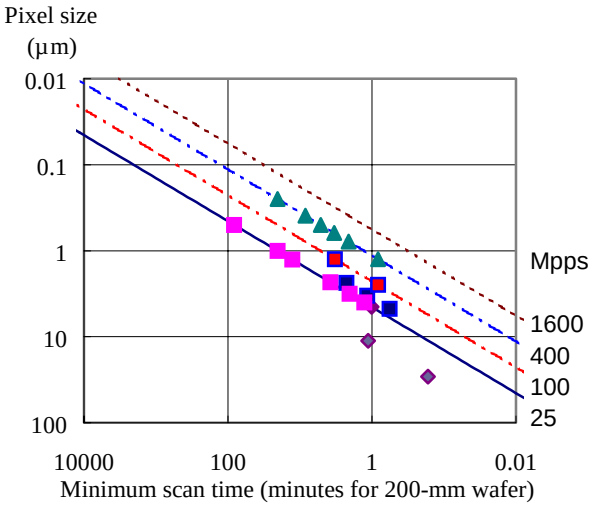

FIGURE 12. Actual inspection time (no overhead) for a 200-mm wafer as a function of pixel size, with pixel rate (Mpps) as a parameter. Points indicate range of some existing systems.

The speed and cost of the image processor for patterned wafer inspection is critical. Fortunately, inspection systems

can leverage off of the improvements in the microprocessor industry. In a sense, we benefit from developments in the same industry we are helping to improve. Computer speeds have improved by ~30% per year over the last three decades (7) and the cost per MIP has fallen by ~65% per year. However, the semiconductor manufacturing industry is increasing the area density of IC devices by 40% per year. Thus, the time it takes for doing the image processing of a wafer should remain approximately constant, even as the required pixel rate needs to increase by 40% per year to maintain throughput. Processing cost should also fall, except for the fact that processing is becoming more complex (more MIPS!).

Classifying defects

In early days of wafer inspection systems classification consisted of reporting a defect size. High resolution, bright-field systems could resolve the defect and determine its area. Dark-field systems, because they detected defects much smaller than the system spot size, measured only the scattering light signal in a single channel. Defect sizing came from comparing this signal against a calibration curve for PSL spheres on the substrate.

For extended defects post-processing algorithms in current systems can classify clusters, scratches, and random defects. For defects smaller than the scanner spot size or the imager optical resolution, however, real time classification requires multiple views or channels. As mentioned in the section on pits vs. particles in this paper, multiple angles of incidence or multiple collection channels provide classification capability. Of course, all this comes at a price because each channel needs support, particularly in image processing.

FUTURE NEEDS AND DEVELOPMENTS

"Predictions are always difficult ....especially about the future." Niels Bohr

Fortunately here we do not have to predict the weather, the stock market, or the economy, all rather chaotic systems. We can predict some evolutionary changes, but revolution is in the minds of inventors. In light of this we'll confine ourselves to some evolutionary changes that will occur.

Smaller critical dimensions, larger wafers and more integrated inspection systems are part of our future. Inspection systems will follow the lead of lithography and migrate to ultraviolet wavelengths. We will also see an even closer coupling of inspection with process equipment, review stations, and yield management systems. However, before briefly discussing these coming developments, we talk about a current gap in inspection, that of inspecting contacts and vias or high aspect ratio structures.

Inspecting contacts and vias

Both optical and SEM inspectors are effective in helping to develop and control IC manufacturing processes. However, there is one major gap in the performance of current systems. It is seeing small defects or residue at the bottom of high aspect ratio structures.

Optically one can detect partially filled or missing contacts in high resolution systems. However, if a residue of 5 nm is at the bottom of a 250 nm diameter by 1000 nm deep via, we are asking the optical system to detect a volume difference equivalent to a 75 nm diameter sphere at the bottom of the hole, a very difficult task (8). Thus, if contact/vias must be checked individually, we are not going to do it optically on real wafers. However, if all the contact/vias within a local area are incompletely etched, then optical means can detect it.

In a SEM system a voltage contrast mode can detect a residue at the bottom of a via or contact. However, SEM inspectors are not fast; thus, to inspect contacts/vias in a reasonable time, we must resort to sampling small areas. Therefore, here again, as with optical techniques, we can observe incomplete etching if this fraction is on the order of roughly 10^{-4}, but finding 5 nm of residue in one contact/via out of 10^{10} of them is beyond practical consideration.

Using UV in inspection systems

For detecting smaller defects bright field systems need the higher resolution of shorter wavelengths. However, in dark field systems the system spot sizes currently employed are not limited by the visible wavelength. Thus, it is not imperative that these systems use UV immediately.

In dark field systems the shorter wavelength of a UV laser leads to a greater scattering cross-section from particles on bare silicon surfaces. That is clear from the Rayleigh "blue sky" factor of λ^{-4}. Therefore, UV systems will be able to detect particles in the range of 20 nm diameter on smooth surfaces

In terms of patterned wafers, however, using UV has the following issues. In dark-field scattering mode operations, one ultimately relies on the phase associated with the interaction of light with the structures. Patterned and unpatterned wafers with films on them will both see a more rapid thin-film effect fluctuation. Thus, process variations across the wafer will have a greater effect with UV illumination. It is, therefore, not obvious that one necessarily gains in detecting defects on dense structures where the amount of scattered power is not an issue. The shorter wavelength will result in the generation of more diffraction orders in the Fourier space to filter out. For larger cell sizes, this also means that the orders are closer together, causing difficulty in removing them. UV optics

and lasers, of course, must be developed and available. For non-PMT detection, UV necessitates tricks such as back-thinning of TDI/CCD detector arrays. UV light also can cause photochemical deposition of air-borne contaminants on the optical surfaces, thus necessitating e.g. a constant nitrogen purge

Even with all of these issues, which can be solved, UV systems will be available in the not too distant future.

Integrated inspection systems

"Time-to-results" is always an important driver in the industry. Thus, we will see more and more integration of inspection hardware units into an overall system that can find the defects, review them, and determine the source of the problem.

The industry has a great incentive to "shorten the loop". As a result there is considerable investigation into bringing metrology and inspection within the process chamber ("in-situ") or into a port on the process equipment. However, both technical and economic barriers exist that make accomplishing this difficult. High performance (sensitivity and throughput) inspection has engineering constraints that make it not easily compatible with process equipment. In addition, the cost of a metrology/inspection module has to be relatively low compared to present-day systems to make it cost-effective. On the other hand, we will see some development of integrated inspection units that are tuned to the specific defects generated by process tools and are sensitive to relatively large defects.

SUMMARY

Wafer inspection system performances have kept up with semiconductor manufacturing industry requirements. Both dark field and bright field systems continue to increase in sensitivity and throughput. To meet future needs these systems will go to higher resolution with faster image acquisition and processing. Real time classification will improve, with better coupling to review, data management, yield learning, and yield management. Ultraviolet wavelength systems will provide an additional increase in capability.

ACKNOWLEGMENTS

We thank Mustafa Akbulut, Kurt Haller, Ning Yin, and Guoheng Zhao for providing us with data and data analyses of pits and particles on silicon wafers.

REFERENCES

1. Bobbert, P. A. and Vlieger, J., *Physica* **137A**, 209-241 (1986)
2. Assi, Fadi Ismail, "Electromagnetic Wave Scattering by a Sphere on a Layered Substrate," Master of Science thesis submitted to the Faculty of the Dept. of Electrical and Computer Engineering, Univ. of Arizona (1990).
3. Stokowski, S. E., Assi, F. I., Cangellaris, A., and Yin, Ning, "Confirming Experimentally the Utility of the Mie-Weyl Formalism for Calculating E-M Scattering by a Sphere on a Layered Substrate", *Proc. 2nd Workshop on Electromagnetic and Light Scattering: Theory and Applications*, Moscow: Moscow Lomonosov State University (1997).
4. Hulst, H. C. van der, *Light Scattering by Small Particles*, New York: Dover Publications, Inc., (1981), p. 432
5. Church, E. L., Jenkinson, H. A., Zavada, J. M., *Opt. Eng.* **18**, 125-138 (1979).
6. Stover, J. C., *Optical Scattering: Measurement and Analysis, second edition*, Bellingham: SPIE Press, 1995.
7. Brenner, A., *Physics Today* **49**, 25 (1996).
8. Socha, Robert J., Neureuther, Andrew R., *J. Vac. Sci. Technol. B* **15,** 2718-2724 (1997).